NANO LETTERS

Letter

pubs.acs.org/NanoLett

Method for Production of Polymer and Carbon Nanofibers from Water-Soluble Polymers

Jonathan Spender,[†,‡] Alexander L. Demers,[†,‡] Xinfeng Xie,[‡,§] Amos E. Cline,[†] M. Alden Earle,[‡] Lucas D. Ellis,[‡] and David J. Neivandt*[,†,‡]

[†]Department of Chemical and Biological Engineering, [‡]Forest Bioproducts Research Institute, and [§]School of Forest Resources, University of Maine, Orono, Maine 04469, United States

Supporting Information

ABSTRACT: Nanometer scale carbon fibers (carbon nanofibers) are of great interest to scientists and engineers in fields such as materials science, composite production, and energy storage due to their unique chemical, physical, and mechanical properties. Precursors currently used for production of carbon nanofibers are primarily from nonrenewable resources. Lignin is a renewable natural polymer existing in all high-level plants that is a byproduct of the papermaking process and a potential feedstock for carbon nanofiber production. The work presented here demonstrates a process involving the rapid freezing of an aqueous lignin solution, followed by sublimation of the resultant ice, to form a uniform network comprised of individual interconnected lignin nanofibers. Carbonization of the lignin nanofibers yields a similarly structured carbon nanofiber network. The methodology is not specific to lignin; nanofibers of other water-soluble polymers have been successfully produced. This nanoscale fibrous morphology has not been observed in traditional cryogel processes, due to the relatively slower freezing rates employed compared to those achieved in this study.

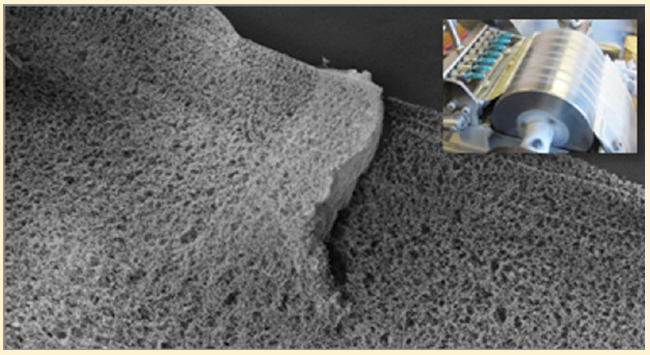

KEYWORDS: *Carbon nanofiber, nanofiber, lignin, ice templating, rapid freezing*

Carbon nanofibers (CNFs) are multifunctional materials of great technological and industrial importance due to their physical, mechanical, and chemical properties.[1−7] They have demonstrated great potential for applications in nanocomposites,[1,6,7] energy storage,[5−7] and catalyst support.[5−7] To date, petroleum-derived polymers, for example, polyacrylonitrile (PAN), and hydrocarbon gases, such as ethylene, have commonly been employed as carbon sources for the production of CNFs.[1−8] However, due to the nonrenewable nature of petroleum resources, it is of great importance to find alternative, sustainable precursors for CNF production.

In an effort to address this issue, the biopolymer lignin has been investigated as a source material to produce CNFs via the adaptation of an existing technology, specifically electrospinning.[9] Lignin exists in the cell walls of all high-level plants. It is the second most abundant natural polymer on earth and is an underutilized byproduct of the pulp and paper industry and the cellulosic bioethanol industry.[10] The majority of lignin removed from biomass is burnt on site for its energy content. Lignin is an attractive precursor for the production of CNFs not only because of its abundance and low value, but also because it has a highly aromatic molecular structure that results in a large carbon mass yield after carbonization when compared to other natural polymers.[11,12] The most frequently investigated method for the production of CNFs from polymeric precursors is electrospinning followed by carbonization.[3,4,9,13] CNFs with diameters as small as 200 nm have been successfully prepared from lignin employing the electrospinning method.[9] However, the use of volatile organic solvents and relatively low processing speeds (several ml of precursor solution per hour) have hindered large-scale production of cost-effective CNFs via this methodology.

Ideally, one would like a CNF production method that employs lignin, is free of organic solvents, and is simple and fast enough to be easily scaled up for commercial production. Here we present a new process that is an extension of the ice-segregation-induced self-assembly (ISISA) methodology.[14]

The ISISA technique involves dissolving or suspending a material (typically, but not limited to, a polymer or monomeric precursor) in water and freezing the solution. As the solution freezes, the growing ice crystals displace and phase separate the polymeric material in an orderly manner, essentially templating the polymer around the ice crystals.[14] The morphology of the ice crystals, and hence the polymer, is dictated in part by the freezing conditions. Contributing factors to the control of the morphology include the freezing rate,[14,15] polymer concentration,[14,16,17] polymer molecular weight,[14,16,17] and volume fraction of the dispersed phase,[17] among others. The frozen

Received: May 25, 2012
Revised: June 15, 2012

   dx.doi.org/10.1021/nl301983d | *Nano Lett.* XXXX, XXX, XXX−XXX

water is subsequently separated from the polymeric matrix, for example, by sublimation. The process has been widely used for the preparation of polymeric scaffolds, for example, chitosan or polyaniline, usually comprising a monolithic, porous, non-fibrous polymer matrix.[16−19] Microfibers have also been produced via this methodology, with typical diameters of several micrometers.[20] A small number of studies have reported production of submicrometer fibers, with average diameters of 500 nm within individual samples.[21−23]

Typical ice templating processes consist of submerging polypropylene vials of the material to be frozen at a constant rate into a cold bath containing a cryogenic fluid.[14,15,20] As the vials are submerged, a freezing front is formed. The submersion rates are typically on the order of centimeters per minute[14,15] and are proportional to the freezing rate.[14,15,20] As the vials are submerged into the cold bath, a gradient in the ice crystal growth rate occurs,[15,24] which correlates with a freezing rate gradient. Higher freezing rates within the material occur physically closer to the cold source, with the rates decreasing as the distance increases due to thermal resistance. The freezing rate gradient leads to variations in morphology throughout the material;[14,15] higher freezing rates generate smaller ice crystals and template smaller polymer morphologies, while lower freezing rates generate larger ice crystals and template larger polymer morphologies.[14,15,25] Higher freezing rates also generate a nonplanar, unstable freezing front.[26,27] The higher cooling rates supercool the solution, resulting in the formation of dendritic ice crystals that are aligned. The solute precipitates around these ice crystals, generating a fibrous structure that has previously been used to generate submicrometer fibers.[21−23]

In previous work performed to generate submicrometer fibers via ice-templating, dilute, polymeric, aqueous solutions were placed in a shallow glass beaker before being submerged into liquid nitrogen.[21−23] The larger area of the sample and smaller thickness promoted faster and more uniform freezing than traditional ISISA methods, although the use of glass as a containment material is problematic due to its low thermal conductivity. As a result, fiber diameters were reduced to the submicrometer range but with considerable variation due to fluctuations in the freezing rate throughout the sample. Our study aimed to dramatically extend the technique of ISISA to produce fibrous polymeric structures with diameters in the tens of nanometer length range with minimal variation in morphology throughout the sample in a readily scalable manner by investigating the impact of very high and uniform freezing rates.

Overall freezing rates are decreased by the presence of a containment vessel, since that material must be cooled and it represents an extra boundary across which heat transfer must occur. Large quantities of solution to be frozen are problematic as cooling rate gradients exist within the sample. Figure 1 illustrates the relationship between templated polymer morphology and freezing rate by presenting a scanning electron micrograph of a lignin solution that was deposited onto a steel surface that had been tempered to 77 K in liquid nitrogen. It is evident from Figure 1 that solution in intimate contact with the cold sink froze rapidly to produce a nanoscale lignin morphology (upper left), while material insulated from the cold sink experienced greater thermal resistance via progressive ice formation and produced a much larger macroscopic polymer morphology due to its slower freezing rate (bottom right). Further, an investigation of Figure 1 reveals that a distinct change in polymer morphology from nanoscale to

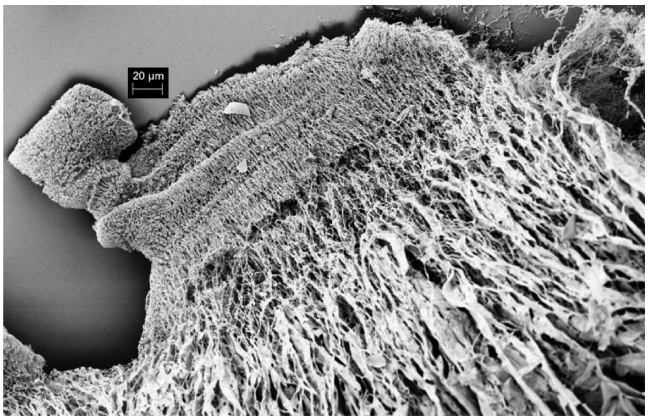

Figure 1. Scanning electron micrograph of a lignin solution deposited on a steel surface tempered to 77 K. A 0.2% (w/w) aqueous lignin solution (Indulin AT, pH 10) deposited via syringe on a steel surface tempered with liquid nitrogen and subsequently lyophilized.

macroscale is observed at film thicknesses of the order of 100−150 μm. As such, it was determined that to ensure rapid, uniform freezing, a film of polymeric (e.g., lignin) solution of the order of 100 μm thickness must be used to minimize the thermal gradient.

Continuous films, with thicknesses of no greater than 130 μm, were produced by delivery of a pressurized aqueous solution at ambient temperature through a 0.254 mm aperture onto a rotating metal drum. The solution would spread to a width of approximately 3 mm upon contact with the drum. Figure 2 presents the rapid freezing device that we designed and constructed for this process. The drum was tempered by liquid nitrogen (applied both internally and externally to the drum) to 77 K (see Supporting Information for detail of the design and operating conditions). The resultant frozen ribbons of material were subsequently lyophilized to liberate the

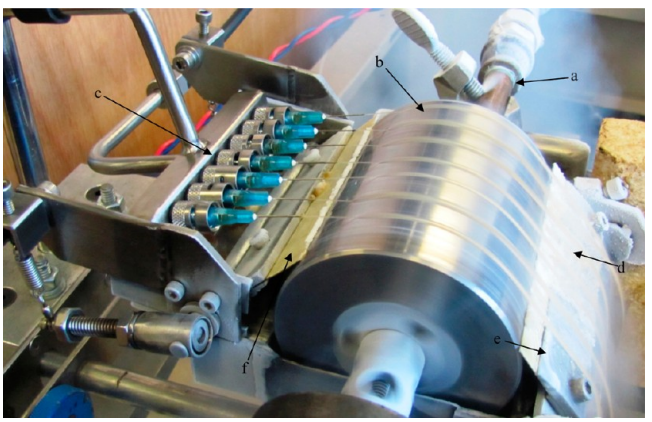

Figure 2. Image of the rapid freezing device for polymeric nanofiber production, depicting a lignin solution contacting the drum, freezing into continuous ribbons, and subsequently being collected in a cold storage vessel. (a) Liquid nitrogen is delivered to the drum from a high pressure tank (1.4 MPa) to maintain the drum at the desired temperature, 77 K. (b) Steel drum is affixed to a variable speed motor (not shown) rotating at ∼300 rpm. (c) Needle manifold delivers polymeric solution to the drum for rapid freezing. (d) Ribbons of frozen solution containing the templated nanoscale polymer matrix. (e) Doctor blade to ensure release of frozen ribbons from the drum. (f) Spring tension loaded wiper blade used to regulate the thickness of the liquid nitrogen layer present on the drum surface.

dx.doi.org/10.1021/nl301983d | *Nano Lett.* XXXX, XXX, XXX−XXX

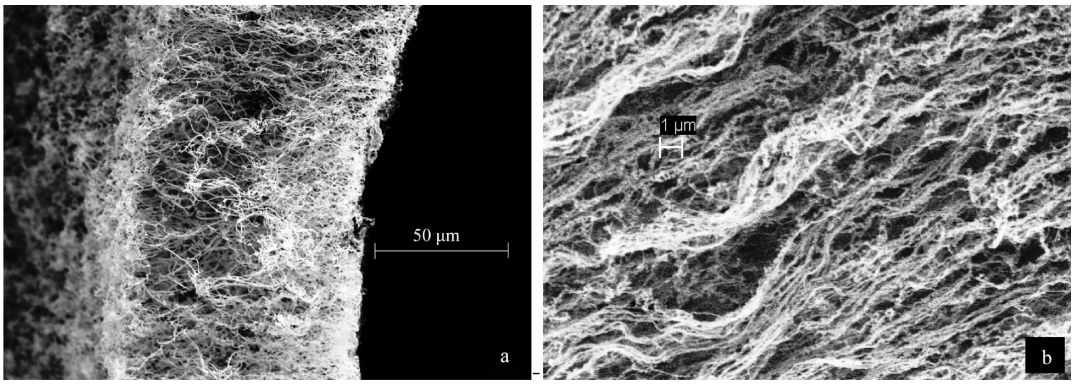

Figure 3. Scanning electron micrographs of nanofibers. (a) SEM of Indulin AT nanofibers templated from a 0.1% (w/w) solution. The scale bar shows a ribbon thickness of approximately 75 μm. Fibers have preferential alignment in the direction of the freezing front, which was normal to the drum surface. (b) SEM of Reax 85A lignin nanofibers templated from a 0.3% (w/w) solution.

templated lignin network (see Supporting Information for the procedure). The freezing of the lignin solution occurred within approximately 0.01 s of initial contact with the drum, as determined by the distance from impact at which a solid ribbon was formed, and knowing the tangential velocity of the drum. An effective cooling rate may be determined by consideration of the energy required to freeze the solution (latent heat of fusion, 335 $J \cdot g^{-1}$ for water),[28] during which no temperature change occurs, and applying that energy to an equivalent decrease in temperature of liquid water (~80 K) using a specific heat capacity of 4.186 $J \cdot g^{-1} \cdot K^{-1}$.[28] Given an ambient solution temperature of 20 K above the freezing point, this calculation results in an estimated cooling rate of 10 000 $K \cdot s^{-1}$. The cooling rate calculated here is less than the 10^6 $K \cdot s^{-1}$ required to vitrify water,[14] so crystalline ice does indeed form.

The resultant ribbons possessed a nanoscale polymeric morphology as determined by scanning electron microscopy (SEM). SEM images showed a fibrous structure with individual fibers having diameters of 100 nm or less and lengths typically greater than 10 μm (Figure 3). The templated material is highly uniform in fiber diameter throughout each sample. Fibers tend to have a preferential alignment in the direction of the freezing front (normal to the drum surface). The concentration dependence of the morphology has been shown to be comparable for a range of water-soluble polymers, including lignin, poly(acrylic acid), carboxymethylcellulose, and polyacrylamide; at concentrations greater than 0.3% (w/w) polymer, large planar structures begin to form in addition to a fibrous network (see Supplementary Figure 1). Consequently, data presented in the current work were produced at concentrations in the range of 0.1−0.3% (w/w). The lignin nanofiber network was subsequently carbonized at 1000 °C to form CNFs (see Supporting Information for the procedure).

Kraft lignin derived CNFs carbonized at 1000 °C were nongraphitic; no characteristic peaks associated with the crystalline domains found in graphite were observed in X-ray diffraction (XRD) measurements. X-ray photoelectron spectroscopy (XPS) analysis indicated that the material contains 92.5% carbon, 5.9% oxygen, and 1.6% sulfur, as calculated from a wide-range XPS scan (see Supplementary Figure 2). The sulfur derives from the fact that the lignin employed was obtained by the kraft pulping process. Oxygen was found to display a single state at 532.6 eV, corresponding to oxygen atoms singly bonded to sp3 carbons. Carbon was found to be present in three states with peaks at 284.2 eV, 285.0 eV, and 287.8 eV, corresponding to condensed aromatic carbon (42.7%), aliphatic carbon (38.5%), and carbonyl carbon (18.8%), respectively.

Adsorption isotherms of nitrogen at 77 K on the CNFs indicated both microporosity and mesoporosity in the material (see Supplementary Figure 3). The steep initial rise of adsorption from a relative pressure of 0.00 to approximately 0.05 is indicative of micropores, while the irreversible hysteresis loop at a higher relative pressure range is associated with mesopores. The analysis indicated a micropore volume of 0.515 $cm^3 \cdot g^{-1}$, accounting for 51.9% of the total pore volume. The mesopore volume was 0.368 $cm^3 \cdot g^{-1}$, accounting for 37.1% of the total pore volume. It follows that 89.0% of the total pore volume was either micro- or mesoporous. The CNF samples had a typical Brunauer−Emmett−Teller (BET) specific surface area of approximately 1250 $m^2 \cdot g^{-1}$ as calculated by the BET equation.[29]

The rapid freezing process described in the present work resulted in the elimination of larger lamellar spaces and macropores observed in other ISISA templates[14−20,25] due to the formation of smaller ice crystals. Much smaller and more uniform fiber diameters were generated than in the glass beaker submersion method[21−23] due to the more rapid heat removal and uniform cooling rates experienced. Indeed, lignin (and subsequently carbon) fibers with diameters of less than 100 nm have been produced (Figure 4), meeting the definition of nanofiber as stated by the International Organization for Standardization in the standard ISO/TS 80004-3:2010. This

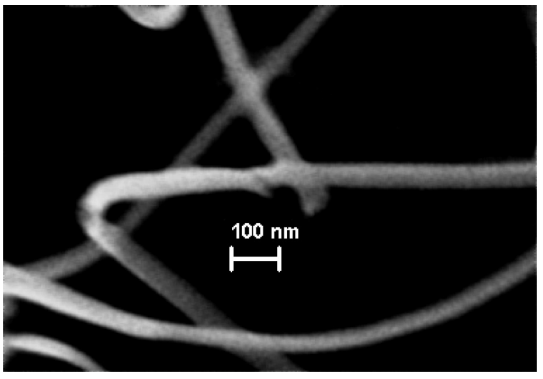

Figure 4. Scanning electron micrograph of carbon nanofibers. Individual CNFs derived from Reax 85A lignin with diameters of less than 100 nm.

dx.doi.org/10.1021/nl301983d | *Nano Lett.* XXXX, XXX, XXX−XXX

method is reproducible, is potentially scalable, and may be applied to the production of CNFs by a wide variety of water-soluble polymers, including the renewable and sustainable biopolymer lignin.

■ ASSOCIATED CONTENT

Ⓢ Supporting Information

Production details for lignin based carbon nanofibers, SEMs demonstrating the effect of concentration on the templated morphology, XPS characterization, and an N_2 adsorption isotherm. This material is available free of charge via the Internet at http://pubs.acs.org.

■ AUTHOR INFORMATION

Corresponding Author

*E-mail: dneivandt@umche.maine.edu.

Notes

The authors declare no competing financial interest.

■ ACKNOWLEDGMENTS

This research was funded by US Army Contract W911QY-10-C-0015, Department of Energy Grant DE-FG02-08ER64625, National Science Foundation Grants EEC-06 48793 and EPS-05 54545, the UMaine Pulp and Paper Foundation, the UMaine Paper Surface Science Program, and the UMaine Forest Bioproducts Research Institute. We thank Dr. Scott Collins and Dr. Christopher Gerbi for SEM analysis, and Dr. George Bernhardt for XPS analysis. We also thank Lauren Wheeler, Sarah Muzzy, Thomas Boyle, Stephanie Yum, Breanne Boutilier, Wilson Adams, and Jeffery Servatas for assistance in the laboratory.

■ REFERENCES

(1) Hammel, E.; Tang, X; Trampert, M.; Schmitt, T.; Mauthner, K.; Eder, A.; Potschke, P. Carbon nanofibers for composite applications. *Carbon* **2000**, *42*, 1153−1158.

(2) Ozkan, T.; Naraghi, M.; Chasiotis, I. Mechanical properties of vapor grown carbon nanofibers. *Carbon* **2010**, *48*, 239−244.

(3) Arshad, S. N.; Naraghi, M.; Chasiotis, I. Strong carbon nanofibers from electrospun polyacrylonitrile. *Carbon* **2011**, *49*, 1710−1719.

(4) Liu, J.; Yue, Z.; Fong, H. Continuous nanoscale carbon fibers with superior mechanical strength. *Small* **2009**, *5*, 536−542.

(5) Zou, G.; Zhang, D.; Dong, C.; Li, H.; Xiong, K.; Fei, L.; Qian, Y. Carbon nanofibers: Synthesis, characterization, and elecrochemical properties. *Carbon* **2006**, *44*, 828−832.

(6) Nataraj, S. K.; Yang, K. S.; Aminabhavi, T. M. Polyacrylonitrile-based nanofibers—A state-of-the-art- review. *Prog. Polym. Sci.* **2012**, *37*, 487−513.

(7) Inagaki, M. *New Carbons: Control of Structure and Functions*; Elsevier: Amsterdam, 2000.

(8) Zussman, E.; Chen, X.; Ding, W.; Calabri, L.; Dikin, D. A.; Quintana, J. P.; Ruoff, R. S. Mechanical and structural characterizaiton of electrospun PAN-derived carbon nanofibers. *Carbon* **2005**, *43*, 2175−2185.

(9) Lallave, M.; Bedia, J.; Ruiz-Rosas, R.; Rodriguez-Mirasol, J.; Cordero, T.; Otero, J. C.; Marquez, M.; Barrero, A.; Loscertales, I. G. Filled and hollow carbon nanofibers by coaxial electrospinning of alcell lignin without binder polymers. *Adv. Mater.* **2007**, *19*, 4292−4296.

(10) Lora, J. H.; Glasser, W. G. Recent industiral applications of lignin: A sustainable alternative to nonrenewable materials. *J. Polym. Environ.* **2002**, *10*, 39−48.

(11) Reed, A. R.; Williams, P. T. Thermal processing of biomass natural fibre wastes by pyrolysis. *Int. J. Energy Res.* **2004**, *28*, 131−145.

(12) Yang, H.; Yan, R.; Chen, H.; Lee, D. H.; Zheng, C. Characteristics of hemicellulose, cellulose and lignin pyrolysis. *Fuel* **2007**, *86*, 1781−1788.

(13) Zhou, Z.; Lai, C.; Zhang, L.; Qian, Y.; Hou, H.; Reneker, D. H.; Fong, H. Development of carbon nanofibers from aligned electrospun polyacrylonitrile nanofiber bundles and characterization of their microstructural, electrical, and mechanical properties. *Polymer* **2009**, *50*, 2999−3006.

(14) Gutierrez, M. C.; Ferrer, M. L.; Monte, F. D. Ice-templated materials: sophisticated structures exhibiting enhanced functionalities obtained after unidirectional freezing and ice-segregation-induced self-assembly. *Chem. Mater.* **2008**, *20*, 634−648.

(15) Mukai, S. R.; Onodera, K.; Yamada, I. Studies on the grouth of ice crystal templates during the synthesis of a monolithic silica microhoneycomb using the ice templating method. *Adsorption* **2011**, *17*, 49−54.

(16) Thongprachan, N.; Nakagawa, K.; Sano, N.; Charinpanitkul, T.; Tanthapanichakoon, W. Preparation of macroporous solid foam from multi-walled carbon nanotubes by freeze-drying technique. *Mater. Chem. Phys.* **2008**, *112*, 262−269.

(17) Whang, K.; Thomas, C. H.; Healy, K. E. A novel method to fabricate bioabsorbable scaffolds. *Polymer* **1995**, *36*, 837−842.

(18) Swetman, L. J.; Moulton, S. E.; Wallace, G. G. Characterisation of porous freeze dried conducting carbon nanotube-chitosan scaffolds. *J. Mater. Chem.* **2008**, *18*, 5417−5422.

(19) Ma, H.; Gao, Y.; Li, Y.; Gong, J.; Li, X.; Fan, B.; Deng, Y. Ice-templating synthesis of polyaniline microflakes stacked by one-dimensional nanofibers. *J. Phys. Chem. C* **2009**, *113*, 9047−9052.

(20) Mukai, S. R.; Nishihara, H.; Tamon, H. Porous microfibers and microhoneycombs synthesized by ice templating. *Catal. Surveys Asia* **2006**, *10*, 161−171.

(21) Qian, L.; Willneff, E.; Zhang, H. A novel route to polymeric sub-micron fibers and their use as templates for inorganic structures. *Chem. Commun.* **2009**, *26*, 3946−3948.

(22) Qian, L.; Zhang, H. Green synthesis of chitosan-based nanofibers and their applications. *Green Chem.* **2010**, *12*, 1207−1214.

(23) Cai, X.; Luan, Y.; Dong, Q.; Shao, W.; Li, Z.; Zhao, Z. Sustained release of 5-fluorouracil by incorporation into sodium carboxymethylcellulose sub-micron fibers. *Int. J. Pharm.* **2011**, *419*, 240−246.

(24) Hottot, A.; Vessot, S.; Andrieu, J. Freeze drying of pharmaceuticals in vials: Influence of freezing protocol and sample configuration on ice morphology and freeze-dried cake texture. *Chem. Eng. Process.* **2007**, *46*, 666−674.

(25) Zhao, K.; Tang, Y.; Qin, Y.; Wei, J. Porous hydroxyapatite ceramic by ice templating: Freezing characteristics and mechanical properties. *Ceram. Int.* **2011**, *37*, 635−639.

(26) Peppin, S. S. L.; Elliot, J. A. W.; Worster, M. G. Solidication of colloidal suspensions. *J. Fluid Mech.* **2006**, *554*, 147−166.

(27) Peppin, S. S. L.; Wettlaufer, J. S. Experimental Verification of Morphological Instability in Freezing Aqueous Colloidal Suspensions. *Phys. Rev. Lett.* **2008**, *100*, 238301.

(28) Eisenberg, D.; Kauzmann, W. *The Structure and Properties of Water*; Oxford University Press: New York, 2005.

(29) Brunauer, S.; Emmett, P. H.; Teller, E. Adsorption of gases in multimolecular layers. *J. Am. Chem. Soc.* **1938**, *60*, 309−319.